Acoustic emission based investigation on the effect of temperature and hybridization on drop weight impact and post-impact residual strength of hemp and basalt fibres reinforced polymer composite laminates

C.Suresh Kumar [a *], Mohamad Fotouhi [b], Milad Saeedifar [c, d], V.Arumugam [e]

[a] *Department of Aeronautical Engineering, Bharath Institute of Higher Education and Research, Selaiyur, Chennai-73, Tamilnadu, India*

[b] *Department of Design and Mathematics, the University of the West of England, Bristol BS16 1QY, UK*

[c] *Non-destructive Testing Lab, Department of Mechanical Engineering, Amirkabir University of Technology, 424 Hafez Ave, 15914, Tehran, Iran*

[d] *Structural Integrity & Composites Group, Faculty of Aerospace Engineering, Delft University of Technology, The Netherlands*

[e] *Department of Aerospace Engineering, Madras Institute of Technology Campus, Chromepet, Anna University, Chennai-44, Tamilnadu, India*

Abstract

This paper investigates the effect of temperature and hybridization on the impact damage evolution and post-impact residual strength of hemp/epoxy, basalt/epoxy and their hybrid laminates, using mechanical and acoustic emission (AE) based analysis. To start with, the specimens were impacted by a drop weight impact tower machine at two temperatures of 30˚C and 65˚C and then they were subjected to a three-point bending test for the assessment of their residual strength, while online AE signals were recorded during the test. The mechanical behavior of the laminates was evaluated through measurement of the impact force and absorbed energy. AE response of the slope of cumulative rise angle (RA) was used for identification of the severity of the impact-induced damage in the laminates. In addition, the sentry function was computed on the basis of the correlation between the mechanical strain energy stored in the materials and the acoustic energy propagates by fracture events, enabled evaluation of the amount of impact-induced damage. These results showed the hybridized laminates having a better resistance to impact damage at the elevated temperature (65^{o}C) compared with the non-hybridized laminates, whereas, in the case of the ambient temperature (30^{o}C), basalt/epoxy laminates had a higher impact damage resistance than other configurations. This study reveals

the capability of the proposed AE-based methods to investigate the effect of temperature and hybridization of composite laminates.

Keywords: Hybrid composites, Impact damage, Elevated temperature, Residual strength, Acoustic emission, Rise angle, Sentry function.

* Corresponding author. Tel: + 91 9486271198, E-mail: sureshmitaero@gmail.com

1. Introduction

Composite materials are widely used in aircraft, spacecraft, ship, automotive and other light-weight structural components due to their superior properties such as higher specific strength, stiffness, long-term durability, better corrosion resistance and excellent fatigue properties. However, laminated composite materials are vulnerable to low velocity impact (LVI) induced damage and this damage may cause their catastrophic failure [1]. During their service life, composites are subjected to various impact loading conditions such as the likelihood of the tool being dropped on the structures during maintenance, strike of a foreign object during takeoff and impact of debris, hailstones or projectiles. Many researchers have attempted the investigation of LVI behavior of composite laminates. In most studies, the effect of various parameters like fibre architecture [2,3], impact velocity and impact geometry [4] have been investigated. Nevertheless, many studies have not reported on the effect of temperature and residual strength estimation of natural fibre hybrid composite laminates under LVI.

Assessment of the effect of temperature on LVI and residual strength of composite laminates are very important, in that their use in load tolerance capability of components exposes them during maintenance operations at relatively higher than ambient temperature. Temperature is one of the key environmental parameters which have a significant effect on the impact response of laminated composite materials [5]. The LVI can notably reduce the stiffness of the composite laminates [6,7] and this LVI gives rise to damages such as interlaminar cracks, matrix cracking, intra-ply crack, delamination and fibre failure [8]. Caprino et al [9] have reported the dependence of residual strength on the extent of delamination and other micro failure that occurred during impact. The effect of temperature ranging from 40^{o}C to 80^{o}C on impact damage resistance of glass/epoxy was investigated by Kang et al [10]. They found temperature having a very small effect on impact damage of laminated composites. Boominathan et al [11] conducted

LVI on carbon/epoxy laminates at elevated (50^{o}C, 75^{o}C and 90^{o}C) and ambient temperatures. They concluded that the residual flexural strength was increased upto 75^{o}C and reduced at 90^{o}C which was close to the glass transition (T_g) temperature. However, there are only a few studies [12] on the effect of temperature on impact-induced damage and evaluation of residual flexural strength for natural fibre hybrid of hemp-basalt composite laminates subjected to impact loading.

Hemp is a naturally ecologically friendly fibre and, after sisal, it is the most widely used natural fibre as reinforcement in composites [13,14]. This natural fibre has acceptable strength and stiffness for use as reinforcement in composite materials. Some advantages and applications of hemp fibre and its composites have been reported by Shahzad [15]. Hemp fibre composites have improved tensile strength, young modulus and better impact performance [16]. Basalt fibre is a natural material composed from volcanic rocks. Continuous basalt fibres can be used as reinforcement in new ranges of concrete and plastic matrix composites. Basalt fibres and basalt-based composites have good thermal properties and can be used in high temperature environments like pipes, bars, fittings, frictional materials, etc. [17]. A number of studies performed, indicate the superiority of the mechanical properties of basalt fibre to glass fibre composites in terms of linear stiffness, young modulus, flexural strength, compressive strength and toughness [18,19] which provides the hybrid composite laminates, the ability to resist higher impact damage than glass fibre laminates [20,21].

Hybridization of different fibres is one of the successful approaches to help increase in the resistance of composite materials against impact damage. Hybrid composites are usually fabricated from two or more different types of fibre reinforced in the same matrix. Petrucci et al [22] have reported the superiority of the flexural modulus of glass/flax/basalt hybrid configuration by 8% and 36% to flax/hemp/basalt and glass/hemp/basalt respectively. In hybrid laminates, optimum mechanical properties were obtained by placing high strength fibres as skin layers [23]. De Rosa et al [24] experimentally found the most favorable degradation pattern for the laminates configuration of lower strength material (glass) as a core and high strength material (basalt) as a skin and slightly less favorable result was obtained using basalt as a core. The poor damage resistance of glass fibre laminates was improved by the hybridization with basalt layers [25]. Better impact strength was obtained for basalt/jute/basalt among different hybrid configurations of basalt and jute fibres [26]. The hybrid effect of hemp and basalt fibre on the flexural and impact strength was investigated for various ratio of hemp/basalt fibre loading [27].

The total fibre loading of the hybrid composites was 40% vol, maximum flexural strength and impact strength was obtained for 0.52:0.48 and 0.68:0.32 hemp/basalt fibre ratios respectively. However, more research studies are still needed for investigation of impact damage progression in natural fibre hybrid composite laminates at elevated temperature.

Nondestructive testing methods have been widely used for the improvement of the damage evolution in laminated composite materials [28]. Acoustic Emission (AE) is a non-destructive testing technique that has good potential for monitoring the damage evolution of composite materials [29-32]. AE signal is the result of transient elastic strain waves generated inside materials as they undergo fracture or deformation. Therefore, this technique is capable of detecting in-situ information relating to the damage mechanisms that occur during loading of composite materials.

Evaluation of the residual tensile strength following the impact of glass/epoxy laminates has been done by AE [33,34] and a damage threshold level was established to identify when mechanical properties of the material started to decreasing. There are also some studies on damage characterization of hybrid composite materials using the AE technique [35-37], showing the potential of this technique for hybrid configurations. Suresh Kumar et al [38] used AE amplitude, duration, counts, energy, rise angle (RA) and peak frequency for characterizing failure modes in hybrid composite laminates. The amount of indentation-induced damage was evaluated in different configurations of carbon, basalt and glass fibres using Sentry function (SF) and Felicity ratio (FR) and RA [39]. A visual correlation was done between the glass/carbon hybrid failure mechanisms in thin-ply composites and the associated AE signals [36]. The cumulative number of AE activity, AE energy, RA and damage indices were used for the assessment of damage progression in glass fibre composites [40]. AE monitoring was used for the identification of the level of damage in hybrid jute/glass-polyester composites during the post-impact flexural tests [41]. AE-based damage characterization in hybrid composites is a challenging task due to the complexity of the damage mechanisms.

A comprehensive damage characterization can be carried out by combining mechanical and acoustical parameters. The sentry function [39,42] which combines both the mechanical and acoustic energy information is a useful tool for this purpose. This function was successfully used for the investigation of fracture energy release rate and damage progression of composite

laminates. Nonetheless, impact damage evolution and post-impact residual properties in natural fibre reinforced composites has only a poor coverage and the impact of their hybrid configurations at different temperatures has been observed. This paper fills the aforementioned gap in literature by applying efficient AE-based characterization methods for the evaluation of the effect of temperature on impact-induced damage and residual strength of hemp/epoxy, basalt/epoxy and their hybrid (hemp/basalt)/epoxy laminates. For that reason, three different status of hemp/epoxy, basalt/epoxy and their hybrid/epoxy composite laminates, with non-impacted and impacted at two different temperatures of 30°C and 65°C, were subjected to a three-point bending load until their failure, alongside on-line monitoring by AE sensors. Later the mechanical data, the AE data and their combination were utilized for the improvement of our understanding about the damage evolution and residual strength estimation of the investigated laminates as shown in Fig.1.

2. Experimental procedures

2.1 Materials

Non-woven hemp fibre mat of 450 g/m^2 and uni-directional basalt fibre of 200 g/m^2 areal weight were used as reinforcement for composite laminate preparations. The thickness as of each layer of hemp fibre and basalt fibre were 0.80±0.05 and 0.19±0.03 mm respectively. Epoxy resin (LY556) i.e., diglycidyl ether of bisphenol-A (DGEBA) with hardener (HY 951) in the ratio of 10:1 was used as the matrix materials.

2.2 Laminates fabrication

The composite laminates were fabricated using hand-layup method. In the case of hemp/epoxy laminate preparation, 4 layers of hemp fibre were heated upto 80^{o}C in an oven prior to laminate preparation for removing the moisture content that helped the bonding between the resin and the fibre system. For the preparation of basalt/epoxy laminates, 12 layers of basalt fibres were aligned in a cross ply orientation of $[0/90/90/0]_{3S.}$ In the case of the hybrid laminate, alternate layers of hemp fibre and basalt fibre configuration of [B/H/B/H/B/H/B]. The fibres were placed on the mold of 50 kN compression molding machine and the resin hardner mix was applied evenly on the fibres by hand-layup process and allowed to cure under a compression pressure of 55 kg/cm^2 at ambient temperature (30^{o}C) for 24 hours. The nominal thickness of all the laminates was maintained as 3.8±0.045 mm. Post curing was performed to ensure a good

adhesion between the fibre and resin. After removal of laminates from the compression molding, they were placed in an oven at a temperature of 65^{o}C for 3 hours. The specimens were cut from the fabricated laminates using a power saw. The dimensions of the specimens were kept as 60 x 60 mm^2 for conducting impact and flexural testing. The fibre weight fraction was 47±3% and the void content was 2.25±0.5% for all laminates. The contents were calculated using a procedure in accordance with ASTM D2734-94 standard.

2.3 Impact testing

The specimens were impacted with an impact velocity of 1.5m/s at two different temperatures of 30^{o}C and 65^{o}C. These values were chosen for the simulation of two different working conditions, 30^{o}C which was around the room temperature and 65^{o}C to simulate a higher temperature which is not higher than the glass transition temperature of the epoxy. For this non-penetrating LVI, Fractovis drop weight impact machine with an environmental chamber was used for conducting the impact test on the specimens as shown in Fig.2. The impacting plunger has a cross-head mass of 1.926kg and the diameter of the hemispherical steel tup was 12.7mm with a clamping force of 1000N. The specimens were impacted with nominal impact energy of 2.17J. This energy level was chosen for causing barely visible impact damage, which is a bigger challenge than a visible impact-induced damage in high-energy levels, due to the difficulty in inspection. Parameters such as impact force, impact energy and deformation were recorded during the conduct of impact tests. Five specimens in each category were used for the test and the average of the results was considered for interpretation.

2.4 Flexural test with AE monitoring

AE software AEWin and an 8 channel AE data acquisition system supplied by Physical Acoustics Corporation (PAC) were used for recording the AE events. Post impact studies were carried out and were assisted by AE monitoring. The sampling rate and pre-amplification were fixed as 3 MSPS and 60 dB respectively. The amplitude threshold was fixed to 45 dB and amplitude distribution covered the range 0-100dB. Nano band piezoelectric sensors (NANO30 PAC sensor) were used as AE sensors for signal accumulation along with high vacuum silicon grease that provided good acoustic coupling between the laminate and the sensor. The sensors S1 & S2 were placed on the laminate 20mm apart from the cross head for signal accumulation as shown in Fig.3. The data acquisition system was calibrated for each kind of laminates. Typical

pencil break test was conducted for the determination of the wave generation at the composite laminate surface and calibration of the sensors. The average wave velocity in the hemp/epoxy was found to be 3020 m/s, the basalt/epoxy to be 3450 m/s and the hybrid (hemp-basalt)/epoxy to be 3200 m/s. The timing parameters were fixed on the basis of the wave velocity obtained. Peak definition time (PDT) for the hemp/epoxy, the basalt/epoxy, and the hybrid (hemp-basalt)/epoxy was determined as 19µs, 17µs and 18µs, respectively. The hit definition time (HDT) is set to 150µs and the hit lock out time (HLT) to 300µs.

3. Results and discussion

3.1 Mechanical Results

The impact force-deformation curves of the laminates are shown in Fig.4. The basalt/epoxy laminates exhibited the highest contact force followed by the hybrid/epoxy and hemp/epoxy laminates. It can be clearly seen that the shapes of the force-deformation histories for the impact test conducted on the basalt/epoxy and the hybrid/epoxy laminates were similar. This was due to the addition of basalt fibre to hemp that improved mechanical strength and therefore the basalt fibre behavior had influence on hybrid/epoxy laminates. The permanent deformation for the basalt/epoxy and hybrid/epoxy laminates was about 0.5 mm and the maximum force occurred at around 2 mm. In the case of hemp/epoxy laminates, the permanent deformation was about 1 mm and the maximum force occurred at around 2.5 mm. The peak force has small reduction for the hemp/epoxy laminates impacted at 65^{o}C compared with 30^{o}C, but negligible changes are observed in the peak force for the basalt/epoxy and hybrid/epoxy laminates. This can be attributed to a significant presence of plasticization or ductile nature of the matrix increasing with temperature.

The absorbed energies for the laminates are shown in Fig.5. It is evident that the absorbed energy has the lowest value for the basalt/epoxy laminates and the highest value for the hemp/epoxy laminates, whereas the hybrid/epoxy laminates have the middle values. Energy absorption in composite materials works through damage creation; therefore, the highest level of absorbed energy in the hemp/epoxy laminates reflects the highest damage creation in these laminates. This is also seen in Fig.4. A noticeable gradient change (non-linearity) and the highest permanent deformation are visible for the hemp/epoxy laminates, which reflect the higher level of damage in this laminate compared to the other laminates.

The impacted and non-impacted laminates were subjected to a three point bending test in the investigation of the effect of temperature and hybridization on flexural after impact strength of the laminates. The resulting flexural strength versus deformation for the investigated samples is shown in Fig.6. The percentage reduction in the residual strength of the laminates impacted at 30^{o}C and 65^{o}C, compared to the non-impacted laminates, is illustrated in Fig.7. The results show a decrease in the residual strength in all the laminates with an increase in the impact temperature. The highest percentage of decrease occurred in the hemp/epoxy laminates, due to the highest impact-induced damage, while lowest one occurred in the hybrid/epoxy laminates. This reveals the hybrid/epoxy laminates having the least impact-induced damage, showing the impact damage resistance of the hybrid composite.

3.2 AE results

Rise angle (RA) value was derived from the division of AE rise time per AE amplitude and has been denoted in "ms/V" unit. Effective performance of RA for identifying the progression stages of damage in the reinforced concrete materials has been reported in [43,44]. Applying a similar concept in this paper; Figs.8, 9 and 10 show stress-deformation and cumulative RA value-deformation curves of the investigated laminates. A comparison of cumulative RA for non-impacted and impacted at different temperatures is also shown in Fig.11. Based on the damage evolution, three different regions with different slopes can be identified in the cumulative RA curves. These slopes were chosen based only on the significant visible changes in the rate of the cumulative RA curves.

In Region I, RA curve has the lowest slope and with no significant active source for AE signals. Therefore it does not have a considerable activated damage mechanism due to the applied load. This region correlates with the linear part of the load-deformation curve and reflects the absence of any change in the stiffness of the laminate. Region II is accordance with appearance of the some significant AE signals that originated from the active damage mechanisms which were responsible for the non-linear behavior of the load-deformation graphs. Region III had the biggest slope, where catastrophic failure occurred in the material through accumulation of the induced damage mechanisms during the tests.

The cumulative RA curve shows different trends for various combinations of layups materials and temperatures that show different forms of failure behaviors in the laminates. For

the hemp/epoxy and basalt/epoxy laminates, trend of the cumulative RA value was increase from the beginning of the load until the final fracture. However, there was no significant increase in the cumulative RA value in Regions I and II. There was a smooth trend (Parabolic shape), making it hard to distinguish Regions I and II from each other. It indicated the failure for the hemp/epoxy and basalt/epoxy laminates having a catastrophic nature and the damage mechanisms appeared mainly in the final stage of the loading, causing sudden and continuous rise in the cumulative RA value trends in Region III. However, in the case of the hybrid/epoxy laminates, significant changes in the trend of cumulative RA value in Region II, which were the result of complex active failure modes in these laminates, due to the effect of the mixed presence of basalt and hemp fibres. For the hybrid/epoxy laminates, the failure had a progressive behavior and it started from the earlier stage of the loading.

For the hybrid laminates, the significant rise in the cumulative RA value is associated with stress levels that are close to the maximum stress levels experienced by the hemp laminates. This shows the presence of some damages in the hybrid configuration, most probably due to the failure of the hemp fibres, when the applied stress in the hybrid configuration reached the failure stress level of the hemp fibres. However the hybrid laminate can tolerate these failure modes unless the stress level reaches a higher value and the basalt fibre starts to fail, which then causes the final failure of the hybrid laminate. The maximum cumulative RA value in the hemp laminates is less than 3000 (ms/V). This value corresponds very well with the cumulative RA value in Region II of the hybrid laminates, supporting the fact that initially the hemp fibres started to fail in the hybrid laminate. This damage mechanism is happening gradually causing stress concentration that leads to failure of the basalt fibres in the hybrid laminates. This can be one reason for slightly lower maximum flexural stress in the hybrid laminates compared with the basalt laminates at which the basalt fibres do not experience any stress concentration and therefore are stronger than the basalt fibres in the hybrid laminates.

Effect of temperature on impact damage was observed from the cumulative RA value trends. The extent of damage to the introduced regions and their trend were different for various combinations of layups materials and test conditions. These differences showed different types of failures in the investigated laminates. Photography of the investigated laminates, taken from the rear side of the non-impacted and impacted surface of the laminates at the temperature of 30^{o}C and 65^{o}C prior to conducting flexural test, is shown in Fig.12. The damage area showed

increase for the case of impacted hemp/epoxy laminates, due to tensile matrix crack, interlaminar crack and fibre fracture. The damage propagation was observed in both the longitudinal and transverse directions which might be due to the lower interlaminar shear strength and impact resistance of hemp fibres. These results were obtained from the lowest cumulative RA and the highest absorbed energy for all the cases of hemp/epoxy laminates compared to other tested configurations.

In the case of basalt/epoxy laminates, only a few localized matrix cracks were found on the rear side faces experienced tension, which initiated an interlaminar crack. This localized matrix crack did not cause any significant reduction in stiffness at 30^{o}C. The initiated interlaminar crack was propagated to barely visible damage for increasing impact force. The absorbed energy showed an increasing trend with respect to increase in impact temperature as depicted in Fig.12. The magnitude of the absorbed energy was at the lower side in comparison with hemp/epoxy and hybrid/epoxy and therefore basalt/epoxy had the highest toughness at 30^{o}C. This result was also evident from the highest cumulative RA value followed by hybrid/epoxy and hemp/epoxy laminates. The failure mechanisms for the basalt/epoxy and hybrid/epoxy laminates were quite similar and had localized matrix cracking and barely visible delamination. Nevertheless, the hybrid/epoxy laminates exhibited a better performance at 65^{o}C which might be due to the polymerization of the matrix. The highest cumulative RA value was obtained for hybrid/epoxy laminates impacted at 65^{o}C. The hybridized system showed a palpable difference in the size of rear surface damage indicating better impact damage resistance at elevated temperature compared to non-hybridized laminates. The susceptibility to impact damage was seen as slightly higher for the investigated laminates impacted at the elevated temperature.

3.3 Damage evaluation using Sentry function

Sentry function provides a comprehensive analysis of the damage evolution, as it combines AE and mechanical results. This function is defined in the logarithm form of the ratio between the mechanical and acoustical energies [30,39,42], as equation 1.

$$f(x) = Ln\left[\frac{E_S(x)}{E_a(x)}\right] \quad (1)$$

where x, $E_S(x)$ and $E_a(x)$ are the displacement, the strain energy and the AE energy respectively.

Based on progress of the damages in the laminates, see Figs.13, 14 and 15, Sentry function has four trends which are as follow:

a) P_I function which is related to the increase in strain energy. Increase in the load caused increase in the mechanical energy and consequently an increase in sentry function. This trend occurs during the first stages of the loading where AE energy is negligible and no significant damage occurs in the laminate.

b) P_{II} function which is related to instantaneous increase of the AE energy and can be seen as a sudden drop trend. The increase in the AE energy is due to a macroscopic damage that occurred in the laminate.

c) P_{III} function is a constant trend and appears when the mechanical energy and the AE energy have equilibrium state.

d) P_{IV} function is a decreasing trend and may happen when the laminate degraded and the damages growth continuously.

Based on the above description, consideration of small P_{II} type function as the occurrence of micro damage in the material, may lead to the consideration of the big P_{II} type functions (big falls) as the macro damage initiation. This is due to the fact that the initiation of the macro damage is a significant internal material damage and as result there is an immediate release of the stored energy which causes an AE signal with high energy content. It can be seen from Figs.13, 14 and 15 that the initiation of macro damage in the laminates has a good correlation with the RA results.

The laminates have different trends in the sentry function curve. For the non-impacted laminates, P_{III} type function appears more than the impacted laminates. But, for the impacted laminates, P_{IV} type function is the dominant type in the sentry function curve. It implies the resistance against evolution of damages more than the impacted laminates following the occurrence of the micro and macro damages within the non-impacted laminate. For the hemp laminates, sentry function trend has almost decreasing trend, P_{IV} type function, which indicates the inability of the laminates to resist against impact-induced damage progression and the

continuous degradation of the laminates and growth of damage. For non-impacted basalt and hybrid laminates, after big fall, P_{III} functions appeared with positive slope showing the capacity of the laminates to tolerate additional strain energy before the final failure. In the impacted laminates and by increasing the temperature, the trend indicated was less observable and there was mostly a decreasing trend after the big fall. A comparison of the basalt and hybrid laminates impacted in 30^{o}C and 65^{o}C, showed some P_{III} functions in the hybrid laminate which meant that the AE energy and the mechanical energy have an equilibrium state. But, for the basalt laminates, P_{IV} functions appear and there is no P_{III} function.

Another interesting result is related to the length of the big fall in sentry function trends. Big falls in the hybrid laminates are clearly larger than the other laminates and length of big fall in the basalt/epoxy laminates is higher than the hemp/epoxy laminates. This indicates the appearance of significant macro failures in the hybrid/epoxy laminates and nonetheless, it has a gradual type of failure occurred in the laminates. Even though the big fall of the hybrid laminates produce a stronger AE signal, but there is still a gradual loss of the strain energy in the laminates due to gradual failure exhibiting the damage tolerant nature of the laminates against impact. But the failures of the hemp/epoxy and basalt/epoxy laminates occur suddenly and they are more susceptible to the impact damage.

Conclusion

This study is meant for the investigation of the influence of temperature and hybridization on impact damage evolution and post-impact residual strength of the hemp/epoxy, basalt/epoxy and their hybrid/epoxy laminates. The investigated laminates were subjected to a three-point bending test and were monitored using AE technique. The mechanical results showed the occurrence of the highest reduction of the residual strength in the impacted hemp/epoxy laminates and the lowest one in the hybrid laminates. In addition, hybrid laminates showed better resistance against impact damage at the elevated temperature compared with the non-hybridized laminates. Different AE trends were observed for each configuration and the AE based methods, sentry function and cumulative RA value, were sensitive enough for the detection of the gradual failure and damage tolerant nature of the hybridized laminates. The conclusion is that hybridization of basalt-hemp fibres improves the resistance to impact and causes a gradual damage evolution. And also this study concluded the sensitivity of AE in the investigation of the

effect of temperature and hybridization on the impact damage resistance of natural fibre reinforced polymer composite laminates.

References

[1]. Ghelli D, Minak G. Low velocity impact and compression after impact tests on thin carbon/epoxy laminates. Compos: Part B 2011; 42:2067-79.

[2]. Atas C, Liu D. Impact response of woven composites with small weaving angles. Inter J Imp Eng 2008; 35:80-97.

[3]. Ghasemnejad H, Soroush V, Mason P, Weager B. To improve impact damage response of single and multi-delaminated FRP composites using natural flax yarn. Mater Des 2012; 36:865-73.

[4]. Mitrevski T, Marshall IH, Thomson R, Jones R, Whittingham B. The effect of impactor shape on the impact response of composite laminates. Compos Struct 2005; 67:139-48.

[5]. Mursakhanov GH, Shchugorev VN. Analysis of temperature and impact damage of fiber reinforced composite. Theor Appl Fract Mech 1994; 20:35-40.

[6]. Choi IH, Kim IG, Ahn, SM, Yeam CH. Analytical and experimental studies on the low-velocity impact response and damage of composite laminates under in-plane loads with structural damping effects. Compos Sci Technol 2010; 70:1513-22.

[7]. Zhang D, Sun Y, Chen L, Pan N. A comparative study on low-velocity impact response of fabric composite laminates. Mater Des 2013; 50:750-56.

[8]. Vieille B, Casado VM, Bouvet C. About the impact behavior of woven-ply carbon fiber-reinforced thermoplastics and thermosetting-composites - A comparative study. Compos Struct 2013; 101: 9-21.

[9]. Caprino G, Lopresto V, Scarponi C, Briotti G. Influence of material thickness on the response of carbon Fabric/epoxy panels to low velocity impact. Compos Sci Technol 1999; 59:2279-86.

[10].Kang KW, Chung TJ, Koh SK. Temperature effect of low velocity impact resistance of glass/epoxy laminates. Inter J Moder Phys B 2010*;* 24: 2657.

[11].Boominathan R, Arumugam V, Santulli C, Sidharth AP, Anand A, Sankar R, Sridhar BTN. Acoustic emission characterization of the temperature effect on falling weight impact damage in carbon/epoxy laminates. Compos: Part B 2014; 56:591-98.

[12].Suresh Kumar C, Arumugam V, Dhakal HN, John R. Effect of temperature and hybridisation on the low velocity impact behavior of hemp-basalt/epoxy composites. Compos Struct 2015; 125:407- 16.

[13].Tong Y, Isaac DH. Impact and fatigue behaviour of hemp fibre composites. Compos Sci Technol 2007; 67:3300-07.

[14].Song Y, Liu J, Chen S, Zheng Y, Ruan S, Bin Y. Mechanical Properties of Poly (Lactic Acid)/Hemp Fiber Composites Prepared with a Novel Method. J Polym Environ 2013; 21: 1117-27.

[15].Shahzad A. Hemp fiber and its composites-a review. J Compos Mater 2012; 46:8973-86.

[16].Kirilovs E, Solizenko R, Kukle S. Specific of hemp fiber's plastic composite projection. Proceed of the 8th Inter Scient Pract Conf 2013; Vol 1:38-56.

[17].Sim J, Park C, Moon DY. Characteristics of basalt fiber as a strengthening material for concrete structures. Compos Part B 2005; 36:504-12.

[18].Lopresto V, Leone C, De Iorio I. Mechanical characterisation of basalt fiber reinforced plastic. Composites: Part B 2011*;* 42: 717–723.

[19].Cerny M, Glogar P, Golias V, Hruska J, Jakes P, Sucharda Z, Vavrova I. Comparison of mechanical properties and structural changes of continuous basalt and glass fibers at elevated temperatures. Ceram - Silikaty 2007; 51:82-88.

[20].Sarasini F, Tirillo J, Valente M, Valente T, Cioffi S, Iannace S, Sorrentino L. Effect of basalt fiber hybridization on the impact behavior under low impact velocity of glass/basalt woven fabric/epoxy resin composites. Compos: Part A 2013; 47:109-23.

[21].Sfarra S, Castanedo CI, Santulli C, Paoletti A, Paoletti D, Sarasini F, Bendada A, Maldague X. Falling weight impacted glass and basalt fiber woven composites inspected using non-destructive techniques. Compos: Part B.2013; 45:601-08.

[22].Petrucci R, Santulli C, Puglia D, Sarasini F, Torre L, Kenny JM. Mechanical characterisation of hybrid composite laminates based on basalt fibres in combination with flax, hemp and glass fibres manufactured by vacuum infusion. Mater Des 2013; 49:728-35.

[23].Nunna S, Ravi Chandra P, Shrivastava S, Jalan A.K. A review on mechanical behavior of natural fiber based hybrid composites. J Reinf Plast Compos 2012; 31:759-69.

[24].De Rosa IM, Marra F, Pulci G, Santulli C, Sarasini F, Tirillo J, Valente M. Post-impact mechanical characterisation of E-glass/basalt woven fabric interply hybrid laminates. Exp Polym Lett 2011; 5:449-59.

[25].Sarasini F, Tirillo J, Valente M, Valente T, Cioffi S, Iannace S. Effect of basalt fiber hybridization on the impact behaviour under low impact velocity of glass/basalt woven fabric/epoxy resin composites. Compos: Part A 2013; 47:109-23.

[26].Amuthakkannan P, Manikandan V, Jappes JTW, Uthayakumar M. Influence of stacking sequence on mechanical properties of basalt-jute fiber-reinforced polymer hybrid composites. J Polym Eng 2012; 32:547-54

[27].Öztürk S. The effect of fiber content on the mechanical properties of hemp and basalt fiber reinforced phenol formaldehyde composites. J Mater Sci 2005; 40:4585-92.

[28].Adams RD, Cawley P. A review of defect types and nondestructive testing techniques for composites and bonded joints. NDT & E Inter 1988; 21:208-22.

[29].Suresh Kumar C, Arumugam V, Sajith S, Dhakal HN, John R. Acoustic emission characterisation of failure modes in hemp/epoxy and glass/epoxy composite laminates, J Nondestruct Eval 2015; 34:1-11.

[30].Fotouhi M and Ahmadi M. Acoustic emission-based study to characterize the initiation of delamination in composite materials. J Thermoplast Compos Mater 2016; 29(4):519-37.

[31].Arumugam V, Suresh Kumar C, Santulli C, Sarasini F, Joseph Stanley A, A global method for the identification of failure modes in fiber glass using acoustic emission. J Test and Eval 2011; 39(5):1-13.

[32].Suresh Kumar C, Pabitha P, Sengottuvelusamy R, Arumugam V, Srinivasan S. Optimization of acoustic emission parameters to discriminate failure modes in glass-epoxy composite laminates using pattern recognition. Struct Health Monit 2018; DOI: 10.1177/1475921718791321.

[33].Caprino G, Teti R. Residual strength evaluation of impacted GRP laminates with acoustic emission monitoring. Compos Sci Technol 1995; 53(1):13-19

[34].Amoroso MP, Caneva C, Nanni F, Valente M. Acoustic emission performance for damage monitoring of impacted FRP composite laminates. Rev Quant Nondestruct Eval 2002; 22:1447-54.

[35].Czigány T. Special manufacturing and characteristics of basalt fiber reinforced hybrid polypropylene composites: Mechanical properties and acoustic emission study. Compos Sci Technol 2006; 66(16):3210-20.

[36].Fotouhi M, Suwarta P, Jalalvand M, Czél G, Wisnom MR. Detection of fibre fracture and ply fragmentation in thin-ply UD carbon/glass hybrid laminates using acoustic emission, Compos Part A 2016; 86:66-76.

[37].Abdou D, Lamine D, Laurent G, Papa BG, Damage detection of a hybrid composite laminate aluminum/glass under quasi-static and fatigue loadings by acoustic emission technique. Heliyon 2019; 5(3): e01414. DOI: 10.1016/j.heliyon.2019.e01414

[38].Suresh Kumar C, Saravanakumar K, Arumugam V. Characterization of failure mechanism in glass, carbon and their hybrid composite laminates in epoxy resin by

acoustic emission monitoring. Nondestruct Test Eval 2019; DOI: 10.1080/10589759.2019.1590829.

[39].Suresh Kumar C, Arumugam V, Santulli C. Characterization of indentation damage resistance of hybrid composite laminates using acoustic emission monitoring. Compos Part B 2017; 111:165-78.

[40].Aggelis DG, Barkoula NM, Matikas TE, Paipetis AS. Acoustic emission as a tool for damage identification and characterization in glass reinforced cross ply laminates. Appl Compos Mater 2013; 20(4):489-03.

[41].De Rosa IM, Santulli C, Sarasini F, Valente M. Post-impact damage characterization of hybrid configurations of jute/glass polyester laminates using acoustic emission and IR thermography. Compos Sci Technol 2009; 69(7-8):1142-50.

[42].Minak G, Morelli P, Zucchelli A. Fatigue residual strength of circular laminate graphite-epoxy composite plates damaged by transverse load. Compos Sci Tech 2009; 69:1358-63.

[43].Ohtsu M, Tomoda Y. Phenomenological model of corrosion process in reinforced concrete identified by acoustic emission. J ACI Mater 2008; 105:194-99.

Ono K, Ohtsu M. Crack classification in concrete based on acoustic emission. Construct Build Mater 2010; 24:2339-46.

Figure Captions

Fig. 1: Summary of the damage characterization and residual strength measurement procedures

Fig. 2: (a) Fractovis instrumented impact tester (b) Impact striker with load cell (c) Specimen held in circular holder and is clamped in environment chamber during impact

Fig. 3: Specimen under flexural loading with AE sensors

Fig. 4: Impacted force versus deformation for hemp, basalt and hybrid/epoxy specimens (a) Impacted at 30^{o}C and (b) Impacted at 65^{o}C

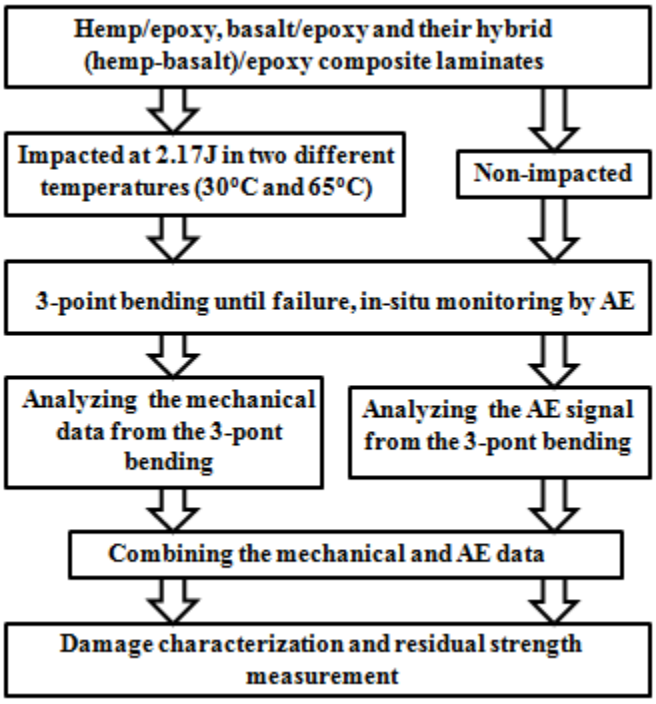

Fig. 1: Summary of the damage characterization and residual strength measurement procedures.

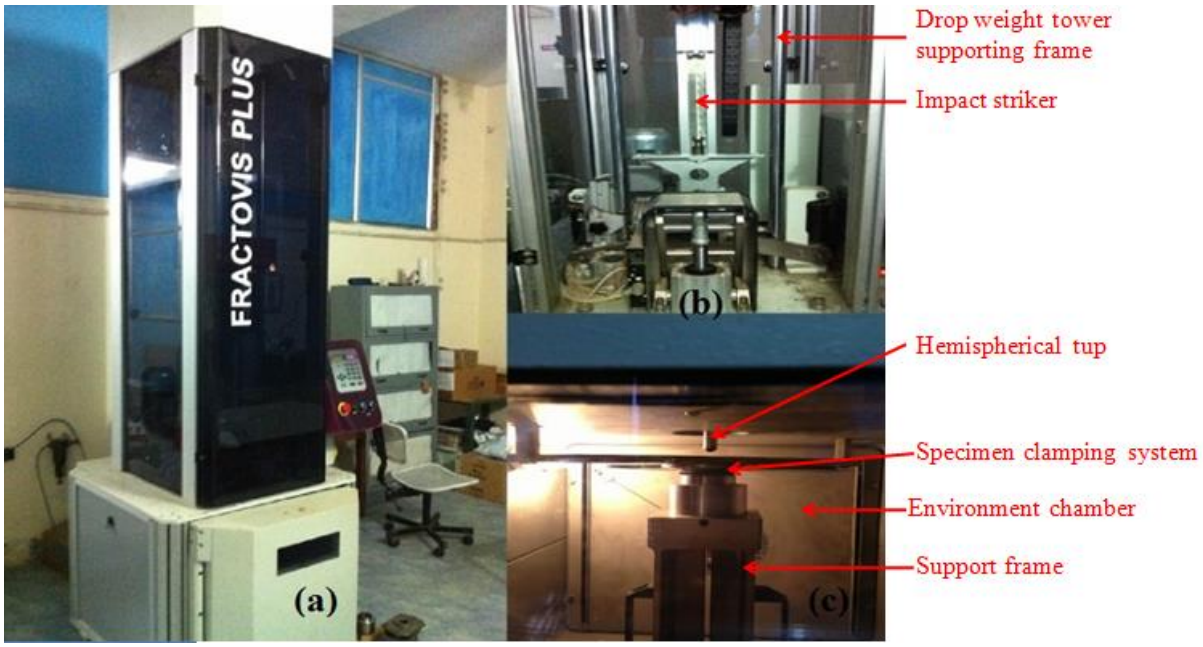

Fig. 2: (a) Fractovis instrumented impact tester (b) Impact striker with load cell (c) Specimen held in circular holder and is clamped in environment chamber during impact

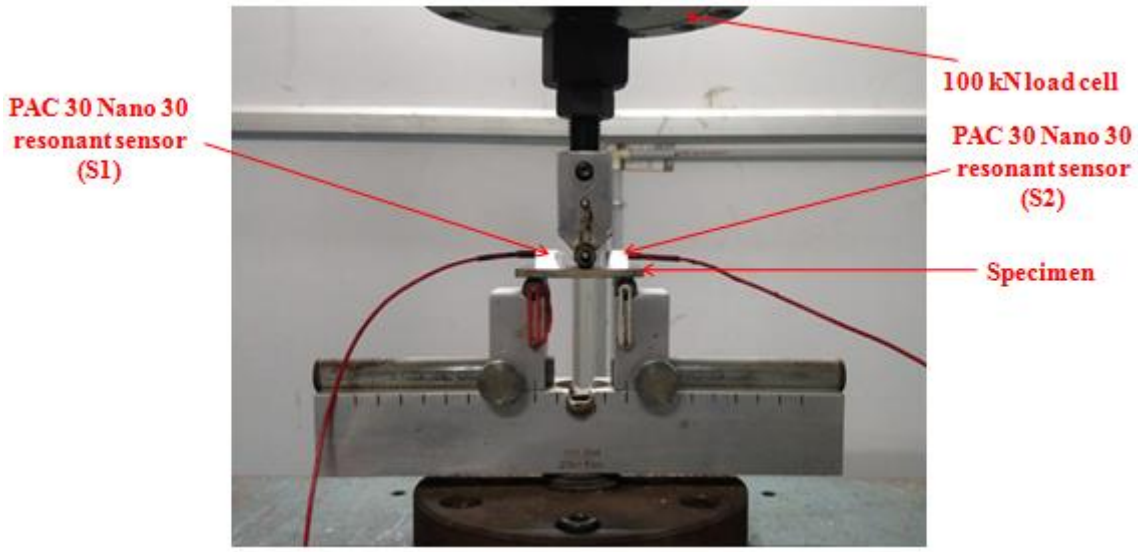

Fig. 3: Specimen under flexural loading with AE sensors

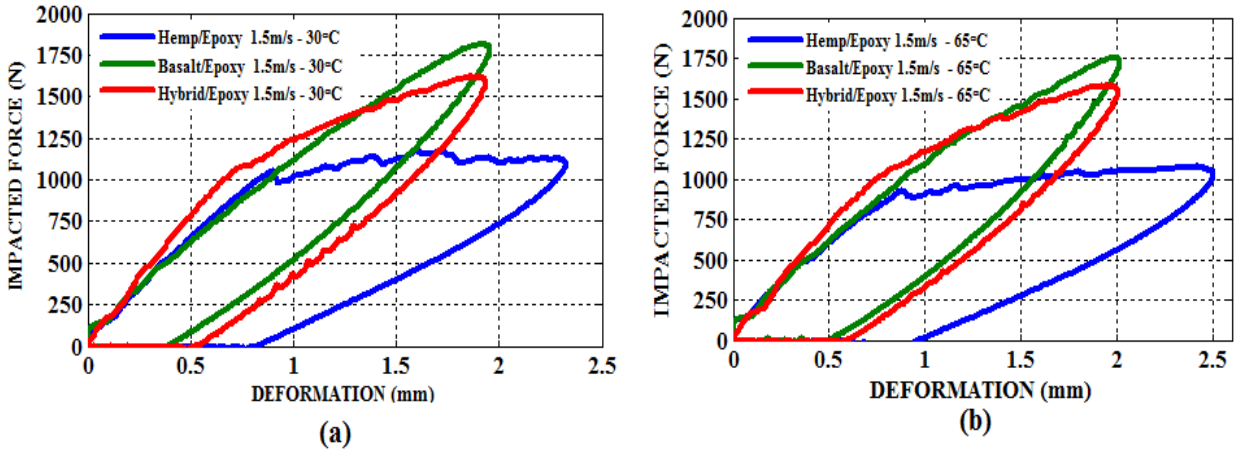

Fig. 4: Impacted force versus deformation for hemp, basalt and hybrid/epoxy specimens (a) Impacted at 30^{o}C and (b) Impacted at 65^{o}C

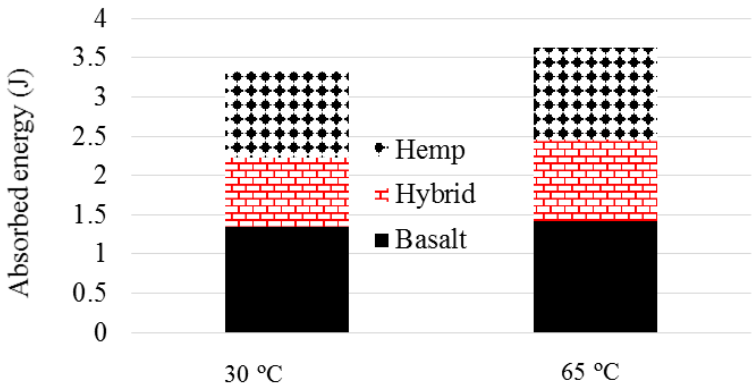

Fig 5: Absorbed energy for hemp, basalt and hybrid/epoxy specimens, impacted at 30°C, and 65°C

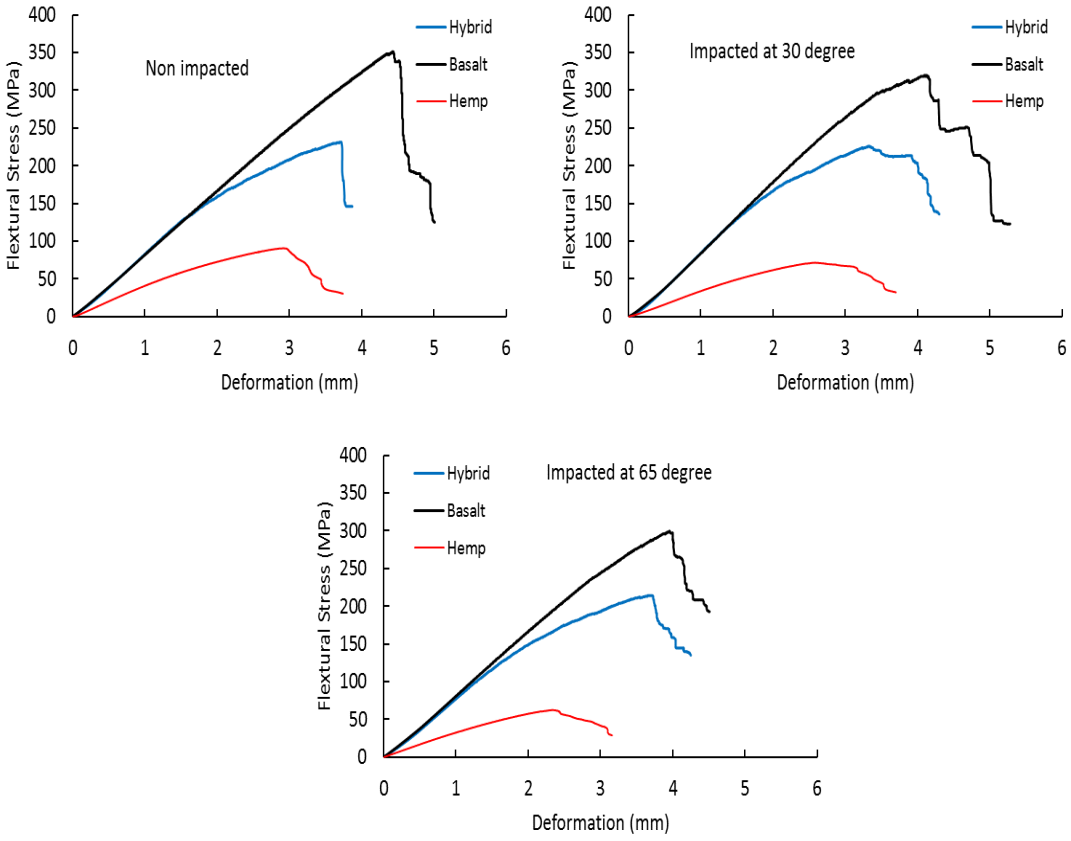

Fig. 6: Flexural Stress versus deformation for hemp, basalt and hybrid/epoxy specimens, non-impacted, impacted at 30°C and impacted at 65°C

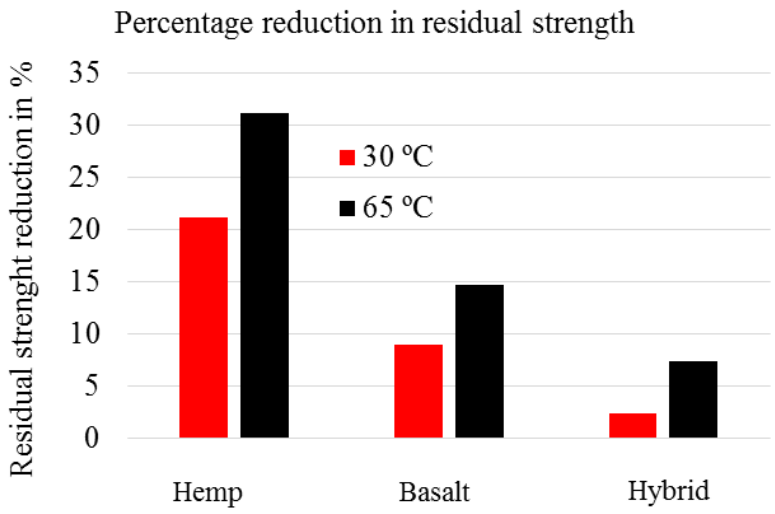

Fig. 7: Residual flexural strength reduction percentage in the laminates

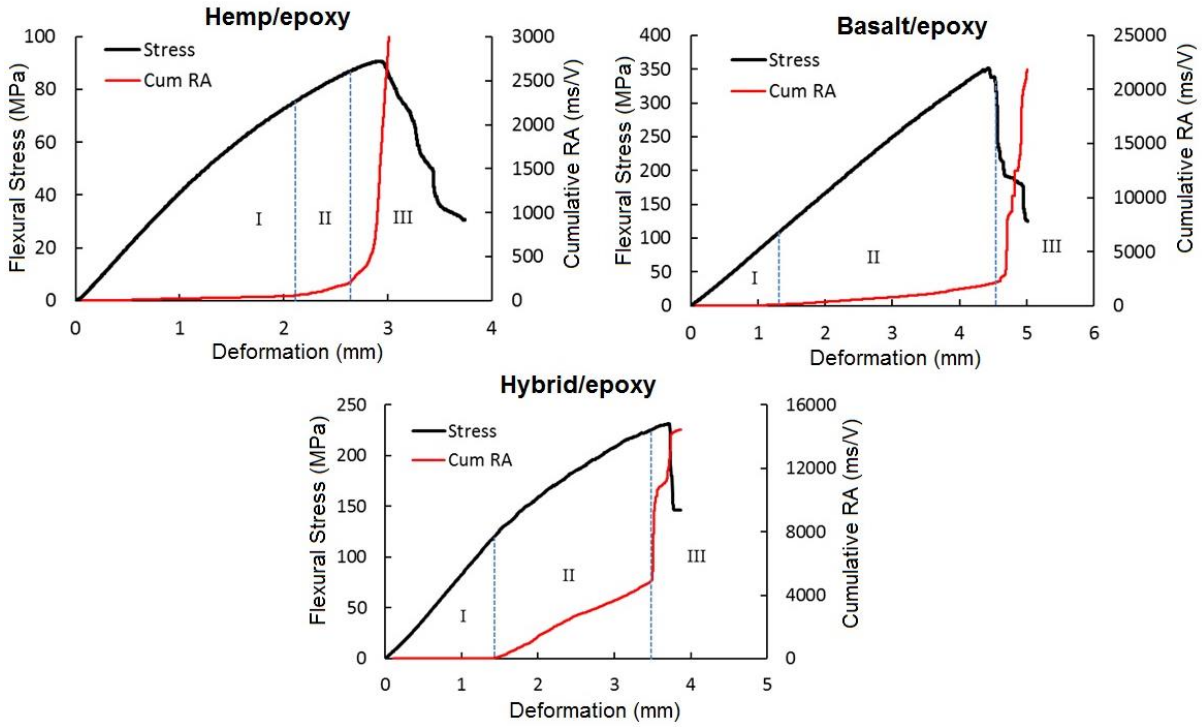

Fig. 8: Stress-deformation and cumulative RA-deformation curves of the non-impacted specimens

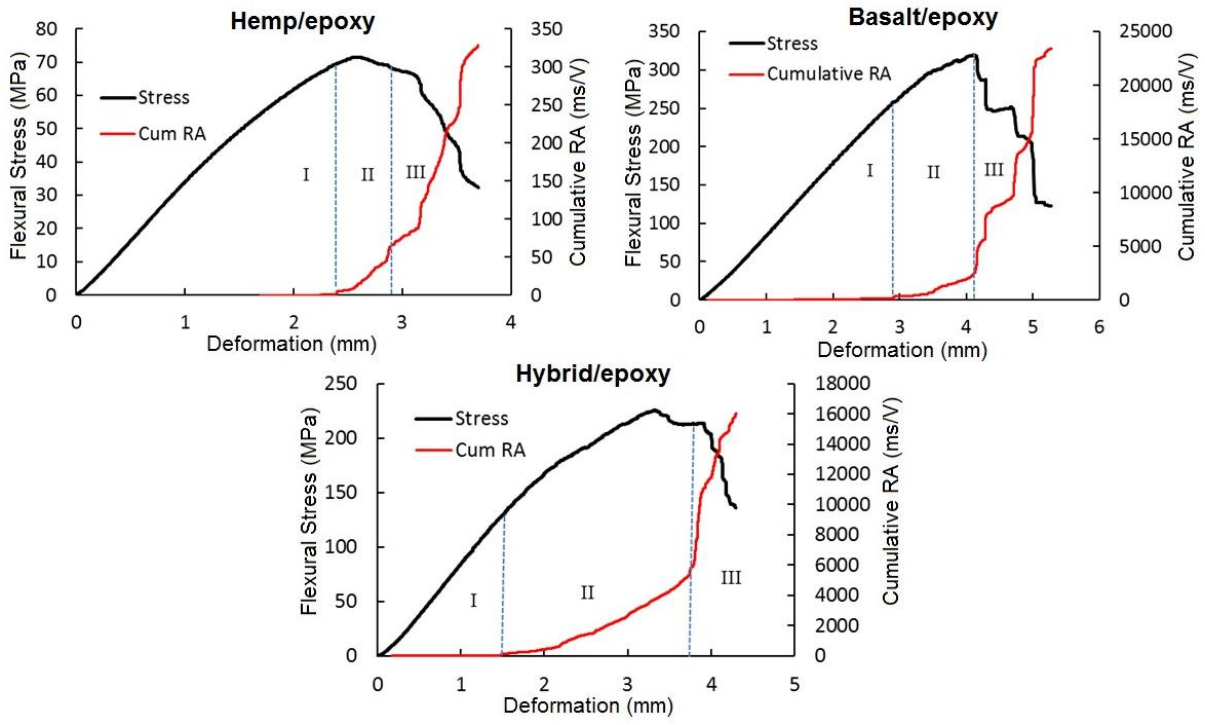

Fig. 9: Stress-deformation and cumulative RA-deformation curves of the impacted specimens at 30°C

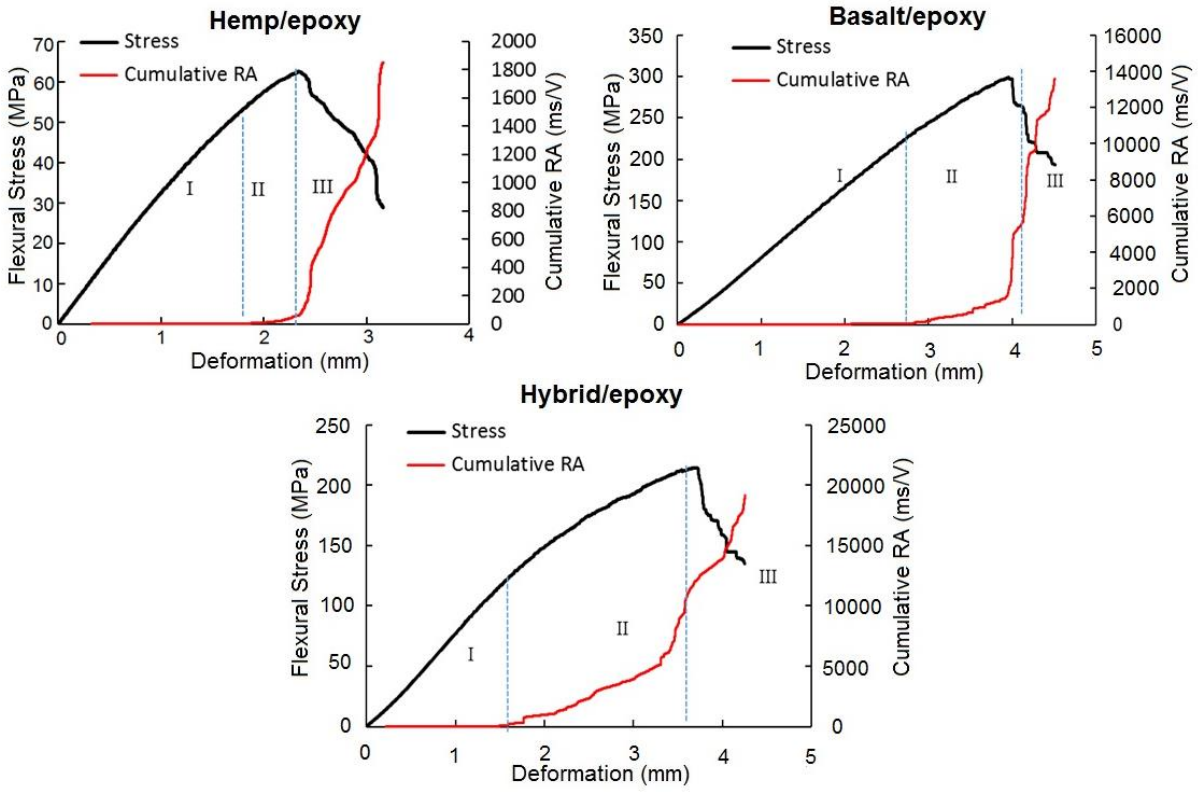

Fig. 10: Stress-deformation and cumulative RA-deformation curves of the impacted specimens at 65°C

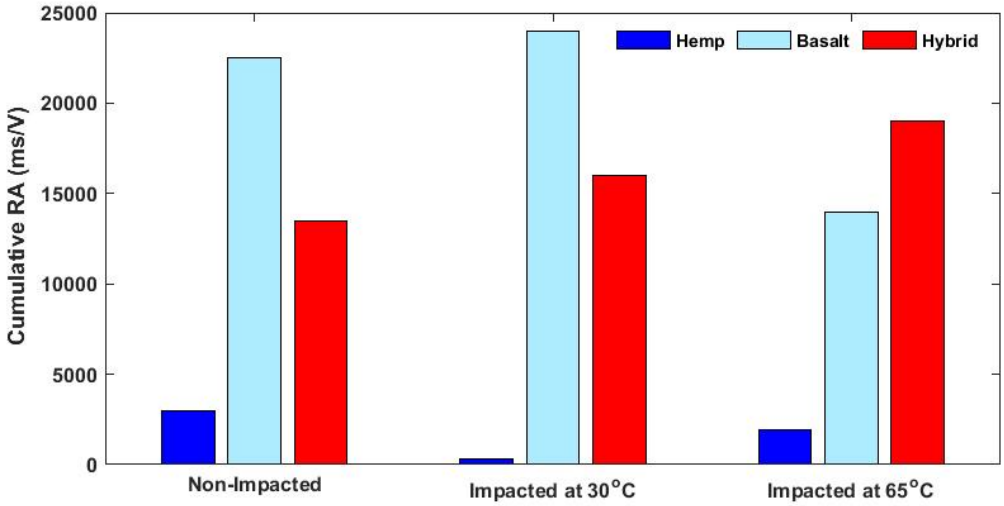

Fig. 11: Comparison of cumulative RA for non-impacted and impacted samples at different temperatures

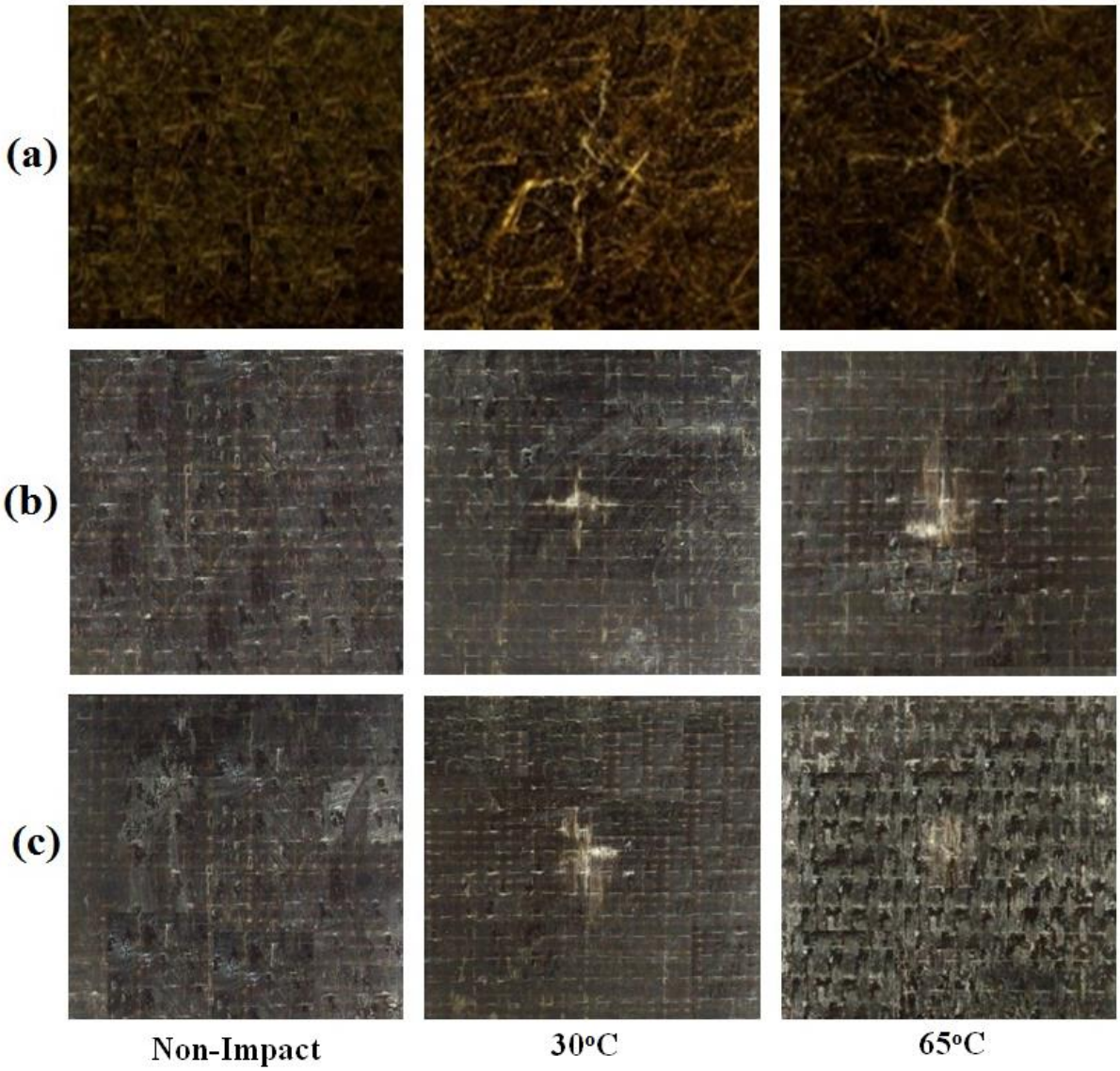

Fig. 11: Rear side photography of (a) hemp/epoxy (b) basalt/epoxy (c) hybrid/epoxy specimens

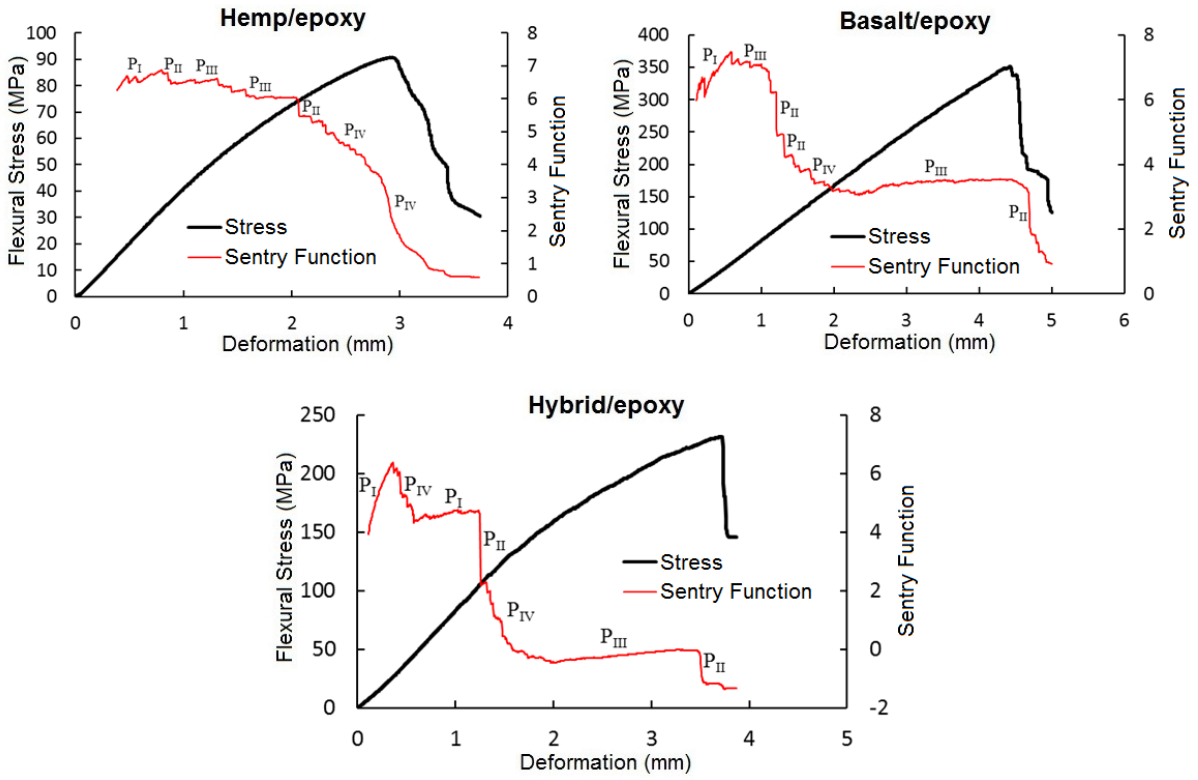

Fig. 13: Stress-deformation and Sentry function-deformation curves of the non-impacted specimens

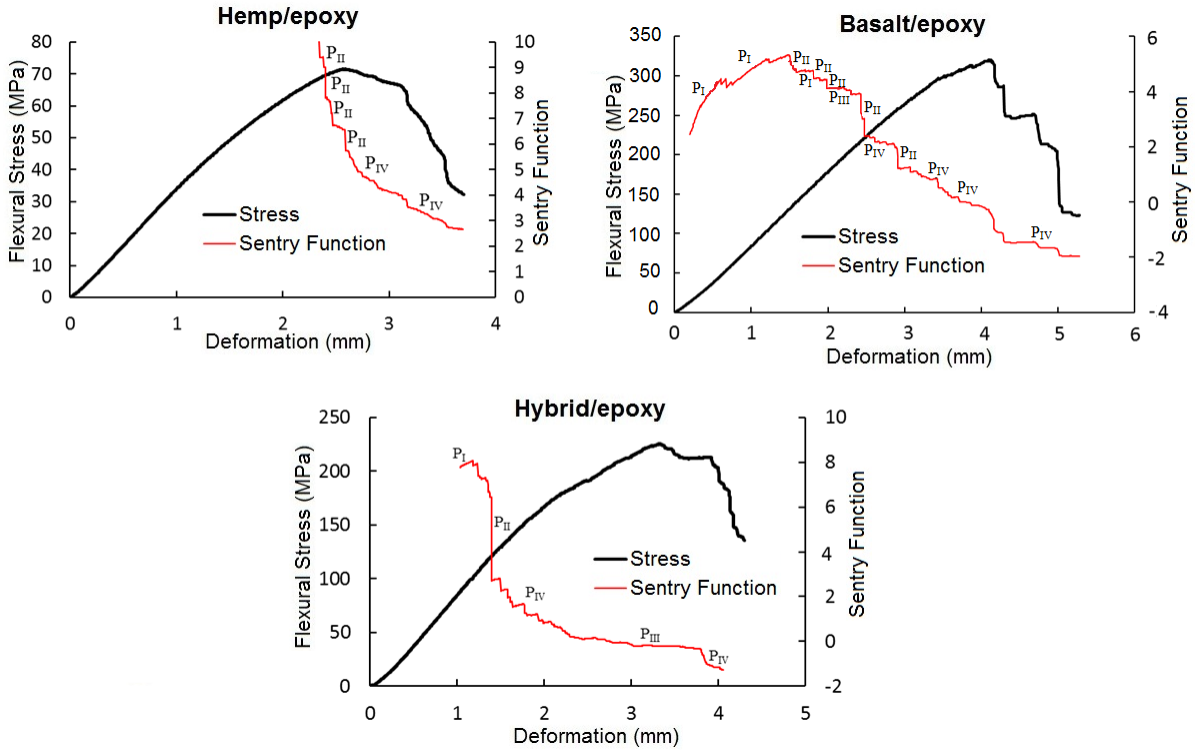

Fig. 14: Stress-deformation and Sentry function-deformation curves of the impacted specimens at 30°C

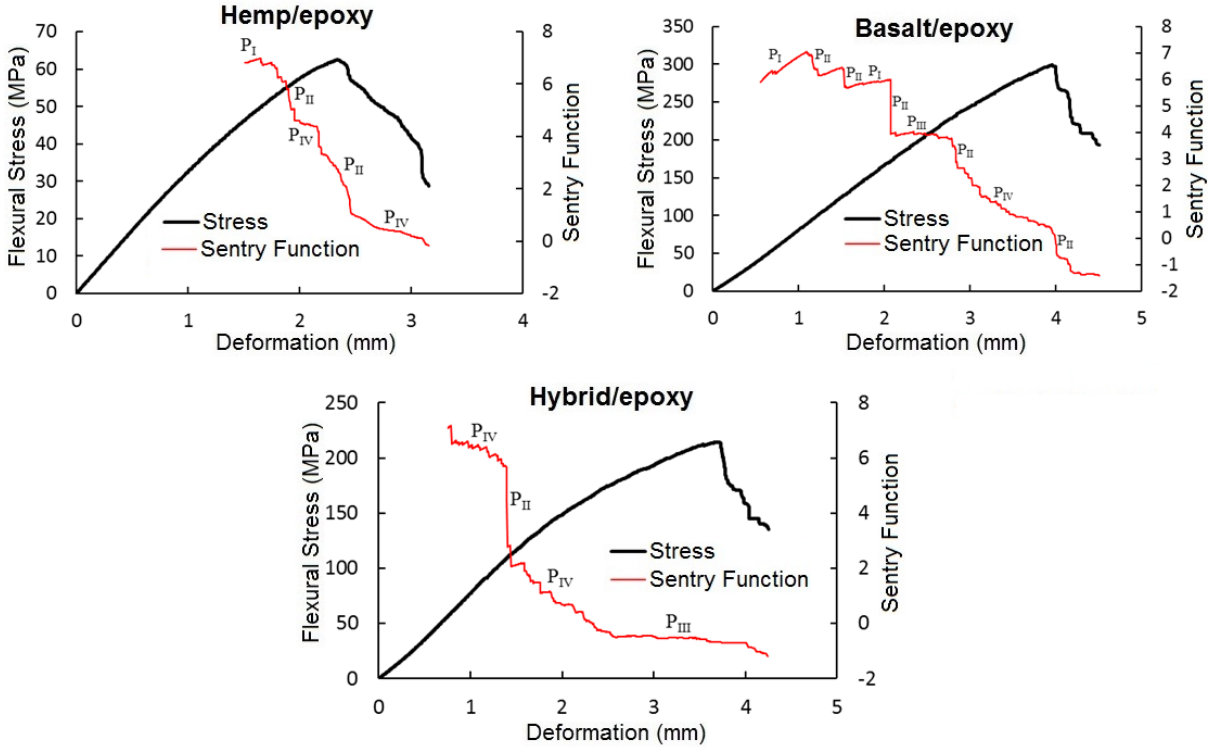

Fig. 15: Stress-deformation and Sentry function-deformation curves of the impacted specimens at 65°C